MRI-visible nanoparticles from hydrophobic gadolinium poly(ϵ-caprolactone) conjugates

Barbara Porsio, Laurent Lemaire, Sarah El Habnouni, Vincent Darcos, Florence Franconi, Xavier Garric, Jean Coudane, Benjamin Nottelet

MRI-visible nanoparticles from hydrophobic gadolinium poly(ε-caprolactone) conjugates

Barbara Porsio[a], Laurent Lemaire[b], Sarah El Habnouni[a], Vincent Darcos[a], Florence Franconi[c], Xavier Garric[a], Jean Coudane[a], Benjamin Nottelet[a]*

[a] Institut des Biomolécules Max Mousseron (IBMM), UMR CNRS 5247, University of Montpellier 1, University of Montpellier 2 - Faculty of Pharmacy, 15 Av. C. Flahault, Montpellier, 34093, France.

[b] Micro et Nanomédecines biomimétiques—MINT, INSERM UMR-S1066, Université Angers, 4 rue Larrey 49933 Angers Cedex9, France.

[c] PRIMEX, Université Angers, 4 rue Larrey 49933 Angers Cedex9, France.

*benjamin.nottelet@univ-montp1.fr

Abstract

In this work we report on the synthesis of two hydrophobic and degradable gadolinium poly(ε-caprolactone) conjugates and their use for the preparation of MRI-visible nanoparticles intended for diagnosis applications. Advantage has been taken from functional poly(ε-caprolactone)s (PCL) bearing propargyl (PCL-yne) or amine groups (P(CL-co-NH_2VL)) to yield conjugates by following two strategies. In a first approach, an azido-chelate of gadolinium (Gd(III)) has been conjugated by CuAAC to PCL-yne to yield a polymeric chelate containing 2.6 wt% of Gd(III). In a second approach, a dianhydride Gd(III)-ligand was reacted with P(CL-co-NH_2VL) to yield, after complexation with Gd(III) salts, a polymeric chelate containing 15.4 wt% of Gd(III). The polymers biocompatibility was assessed against L929 fibroblasts. In a second part, advantage was taken from the PCLs conjugates hydrophobicity to easily prepare by nanoprecipitation nanoparticles with diameters ranging from 120 to 170 nm. The nanoparticles MRI-visibility was then evaluated and confirmed under the spin-echo and the clinically relevant gradient-echo MRI sequences.

Keywords: nanoparticles, MRI, polyester.

1. Introduction

Magnetic resonance imaging (MRI) is the leading imaging technique to provide high spatial and temporal resolutions in clinical diagnosis and enhance the detection and characterization of lesions within the body.[1] In this frame, MRI-visible nanoparticles are proposed for early tumor diagnosis (especially in liver), thrombus diagnosis, as well as for their potential as platform for multifunctional biomedical applications with simultaneous drug-delivery and imaging capabilities.[2,3] Polymeric nanoparticles are generally associated with negative contrast agents (CAs), that contain ferrous superparamagnetic compounds (T2/T2* agents), or positive CAs, that contain paramagnetic elements (e.g., gadolinium Gd(III)) (T1 agents), embedded or grafted to the materials. T1 agents are however generally preferred over T2/T2* agents as they induce a positive enhancement of the signal by modulating the longitudinal relaxation time of the water protons in the tissues.[4] This explains why the blood pool agents currently approved for clinical uses are mainly based on hydrophilic and low molecular weight Gd(III) chelates (Magnevist®, Dotarem®, Omniscan™) that are injected prior to MRI scanning in order to increase the signal. However, large amounts of these potentially toxic contrast agents are needed per injection.[5] Various strategies have therefore been proposed to address this problem in particular with water soluble macromolecular contrast agents (MMCAs) that are known to remain in the vascular system for a longer period, and may thus provide a longer imaging window and a more favorable signal-to-noise ratio. In addition, polymeric systems are believed to allow higher sensitivity by increasing the relaxivity of Gd(III)-CAs and allow modulating the pharmacokinetics of Gd(III)-CAs.[6]

More in details, a common strategy to get higher relaxivity relies on the reduction of Gd(III)-CAs tumbling rate in solution. This can be obtained by the design of polymeric systems whose higher conformational rigidity over low molecular weight chelates is expected to restrict the internal rotation of the Gd(III)-CA.[7] MMCAs with multiple Gd(III) centres have

thus extensively been studied,[4, 8, 9] and include water-soluble polycondensates of chelates,[10-13] water-soluble linear, brush, star or dendrimer conjugates,[14-20] or amphiphilic copolymeric conjugates able to self-assemble into the form of core-shell micelles.[21-26] However, one drawback resides in the limited relaxivity enhancements because of the flexibility of the copolymers used, especially poly(ethylene oxide), and the fact that Gd(III) centers are in most cases linked as chain-ends moieties, which limits their conformational restriction. In that sense, crosslinked structures can be an interesting alternative to slow down Gd(III) centers rotational motions.[27] The use of hydrophobic polymer backbone bearing Gd(III) centers to generate MRI nanoparticles may be another alternative as recently illustrated by our group.[28-30] Indeed, although hydrophobic environment do not favor the formation of hydration sphere and water molecule exchanges between the inner and second hydration sphere, it could be of benefit to provide a more constraint environment.[31] This approach is to date limited to the use nanoparticles made of FDA approved hydrophobic, non-cytotoxic and biodegradable polyesters like PLA and PLGA to encapsulate Gd(III) chelates. However, hydrophilic low-molecular weight Gd(III) chelates incorporated into PLGA micro- or nanospheres have been shown to rapidly diffuse out leading to a loss of MRI-visibility.[2,31-34] To avoid this, surface modification of PLGA nanospheres was recently proposed by Ratzinger et al. who immobilized diethylenetriaminepentaacetic acid (DTPA) and 1,4,7,10-tetraazacyclododecane-1,4,7,10-tetraacetic acid (DOTA) ligands on spacers prior to Gd(III) chelation.[35] Although very promising, two main drawbacks were reported. First, Gd(III) final dose was highly dependent on the type of ligation, with efficient loading obtained only with poly(ethylenimine) spacers leading to core-shell amphiphilic structures. Second, extensive washes had to be performed by successive dialyses to eliminate the non complexed Gd(III) which resulted in partial degradation of the PLGA particles.

The present work aims at an alternative strategy for the preparation of MRI-visible nanoparticles directly generated from original multivalent PCL-based MMCAs. By contrast with others MMCAs, we take advantage of two multifunctional PCLs, namely a propargylated PCL and an aminated PCL, to yield hydrophobic PCL-based multicenters MMCAs by Cu^{I}-catalyzed [3+2] cycloaddition (CuAAC) and amidification reaction, respectively. MMCAs are characterized in particular with respect to their Gd(III) content and their cytocompatibility. Thanks to their hydrophobicity, the PCL MMCAs are then used to easily prepare MRI-visible nanoparticles that are characterized in terms of size and surface charges. Finally, the nanoparticles MRI-visibility is evaluated *in vitro* under the spin-echo and the clinically relevant gradient-echo MRI sequences.

2. Materials and methods

2.1 Materials

Benzyl alcohol, ε-caprolactone and toluene were dried over calcium hydride for 24 hours at room temperature and distilled under reduced pressure. Tetrahydrofuran (THF) was dried by refluxing over a benzophenone-sodium mixture and distilled. All other chemicals were obtained from Aldrich and were used without any further purification. Deuterated chloroform ($CDCl_3$) and dimethyl sulfoxide ($DMSO_{6D}$) were purchased from Eurisotop (Saint-Aubin, France). Spectra/Por dialysis tubes (cut-off 1000, 3500, 5000 g/mol) were purchased from Spectrum Labs (Breda, The Netherlands). PrestoBlueTM, Dulbecco's Modified Eagle Medium (DMEM ⁄ F-12), Phosphate Buffered Saline (PBS), sterile Dulbecco’s Phosphate Buffered Saline (DBPS), Foetal Bovin Serum (FBS), penicillin, streptomycin, and glutamine were purchased from Invitrogen (Cergy Pontoise, France). BD Falcon™ Tissue Culture Polystyrene (TCPS) 24-well plates were purchased from Becton Dickinson (Le Pont de Claix, France).

2.2 Characterization

^{1}H NMR and ^{13}C NMR spectroscopy was performed on a Bruker spectrometer (AMX300) operating at 300 MHz and 75 MHz, respectively. Deuterated chloroform or deuterated dimethyl sulfoxide were used as solvents. Chemical shifts were expressed in ppm with respect to tetramethylsilane (TMS).

Infrared spectroscopy was performed on a Perkin Elmer Spectrum 100 FT-IR spectrometer using the attenuated total reflectance (ATR) technique.

Size exclusion chromatography (SEC) was performed at room temperature on a Waters system equipped with a guard column, a 600 mm PLgel 5 mm Mixed C column (Polymer Laboratories), and a Waters 410 refractometric detector. Calibration was established with poly(styrene) standards from Polymer Laboratories. THF was used as eluent at a flow rate of 1 $mL.min^{-1}$.

LC/MS analyses were performed on a Q-TOF (Waters) spectrometer fitted with an electrospray interface. Solvents used for HPLC and LC/MS were HPLC grade. MALDI analyses were performed on a Ultra-Flex III (Bruker) spectrometer using a dithranol matrix.

Gd(III) quantification was performed on an Element XR sector field ICP-MS (inductively coupled plasma-mass spectrometry) at Géosciences in Montpellier (University Montpellier II). Internal standardization used an ultra-pure solution enriched with indium.

Particle size and zeta potential determination were performed on a Zetasizer Nano ZS (Malvern Instrument, UK). For mean particle size and polydispersity index (PDI) measurements, the samples were diluted in milliQ water. For zeta potential analyses, the

samples were diluted in milliQ water or PBS (pH = 7.4). Solutions were filtered through a 0.45µm filter. All measurements were performed in triplicate.

Transmission electron microscope (TEM) micrographs were obtained with a JEOL 1200 EXII (working voltage of 120 kV). A drop of nanoparticles solution was placed onto a carbon-supported copper grid for 5 min. The excess liquid was removed by capillarity with a filter paper. Mean particle size was determined by measuring the particles diameter with Image J software (Rasband, W.S., ImageJ, U. S. National Institutes of Health, Bethesda, Maryland, USA, http://imagej.nih.gov/ij/, 1997-2012)

2.3 Synthesis of MRI-visible P(CL[DTPA(Gd)]) **3**

3 was prepared by reaction between poly(α-propargyl-ε-caprolactone-*co*-ε-caprolactone)s P(Pg-CL) **2** ($F_{\alpha Pr\varepsilon CL}$ = 5%, Mn_{SEC} = 25000 g.mol^{-1}. Đ= 1.9) and a clickable Gd(III) chelate (diN_3-DTPA(Gd(III))) **1** (full synthetic details for compounds **1** and **2** can be found in the Supporting Information). Briefly, copolymer **2**, complex **1** (3 eq./αPgεCL units) and CuBr (2eq./αPgεCL units) were solubilized in a large amount of dimethylformamide (DMF). The solution was degassed by three freeze-pump-thaw cycles. N,N,N′,N″,N″-pentamethyldiethylenetriamine (PMDETA) (2eq./ αPgεCL units) degased by argon bubbling was added to the reaction medium. The reaction was carried out for 48 hours at room temperature under stirring. The crude medium was dissolved in THF for dialysis (CO 3500 g.mol^{-1}) against distilled water. **3** was recovered after removal of the solvents and dried *in vacuo*. The content of complexed Gd(III) in **3** was quantitatively determined by ICP-MS : 2.6 wt%.

2.4 Synthesis of MRI-visible P(CL-co-VL[DTPA(Gd)]) **5**

5 was prepared by reaction between poly(ε-caprolactone-*co*-5-amino-δ-valerolactone) P(CL-*co*-NH_2VL) **4** ($F_{NH2–VL}$ = 33%, Mn_{SEC} = 6000 g.mol^{-1}. Đ= 1.2) and DTPA dianhydride (full synthetic details for compound **4** can be found in the Supporting Information). More in details, a solution of DTPA dianhydride (162.1 mg, 1.2 eq. with respect to NH_2 groups) in anhydrous DMF was added dropwise to a solution of **4** (100 mg, 0.37 mmol of NH_2) in a large amount of anhydrous DMF (4 mL) and in the presence of triethylamine (0.1 mL; 3eq. with respect to NH_2 groups). The reaction was left to stir for 24 hours at room temperature under an inert atmosphere of argon. The resulting polymer was purified by dialysis against an HCL solution (0.1M) and distilled water (CO 1000 g.mol^{-1}). The polymer was finally recovered by freeze-drying in good yield (205 mg). The extent of amidification was determined by ^{1}H NMR analysis (60% yield).^{1}H NMR (300 MHz; DMSO-d_6), δ (ppm): 4.00 (m, -C*H*$_2$-O)$_{NH\text{-}VL\ \&\ \varepsilon CL}$, 3.75 (CH$_2$-C*H*(NH$_2$)-CH$_2$)$_{NH\text{-}VL}$, 3.60-3.00 (N-C*H*$_2$, CH$_2$-C*H*(N)-CH$_2$)$_{NH\text{-}VL\ \&\ DTPA}$, 2.20-2.40 (CO-C*H*$_2$-CH$_2$)$_{NH\text{-}VL\ \&\ \varepsilon CL}$, 1.70 (CH$_2$-C*H*$_2$-CH(N))$_{NH\text{-}VL}$, 1.30-1.60 (CH$_2$-C*H*$_2$-CH$_2$-C*H*$_2$-CH$_2$)$_{\varepsilon CL}$.

Complexation of the macromolecular ligand with Gd(III) was then carried out. In a typical experiment, the copolymer (100 mg, 9.3×10^{-5} mol of mono-amide DTPA) was solubilized in DMSO (5 mL) before addition of $GdCl_3$-6H_2O (63 mg, 1.9×10^{-4} mol, 2eq. with respect to mono-amide DTPA). Complexation was let to run for four days under stirring at 40 °C. The polymer was purified by dialysis (CO 1000 g.mol^{-1}) against methanol for 24 hours before final recovery of **5** by solvent removal under reduced pressure. The content of complexed Gd(III) in **5** was quantitatively determined by ICP-MS : 15.4 wt%.

2.5 Preparation of MRI-visible nanoparticles

Nanoparticles were prepared with a concentration of Gd(III) of 0.1 wt% with respect to PCL. In a typical experiment, 477.5 mg of PCL (Mn_{SEC} = 35 000 g/mol, Đ = 1.86), 22.5 mg of **3** and 180 mg of SPAN®80 were dissolved in 90 mL of acetone. This organic solution was added dropwise to an aqueous phase containing Tween®80 (360 mg in 180 mL) under magnetic stirring and at room temperature. The mixture was left under stirring for 2 hours to form the nanoparticles by solvent diffusion. Acetone and part of the water were eliminated at 30 °C under reduced pressure to a final suspension volume of 100 ml. The suspension was dialyzed for 24h against distilled water (CO = 5 000 g/mol) before freeze-drying and recovery of the nanoparticles (**NP3**) in good yield (83%).

Similar conditions were used to prepare nanoparticles (**NP5**) from polymer **5** with adjusted ratios of PCL and **5**.

2.6 MR imaging protocols

MR imaging experiments were performed on a Bruker Biospec 70/20 system operating at a magnetic field of 7T (Bruker, Wissembourg, France). The resonant circuit of the NMR probe was a 35-mm diameter birdcage resonator. MRI nanoparticles, under the form of small clusters, were embedded in a degassed 1 % (w/w) agarose gel prior to imaging. To test signal enhancement, samples were analyzed using either a three-dimensional (3-D) acquisition with relaxation enhancement (RARE) sequence (TR = 3000 ms; mean echo time (TEm) = 8 ms; RARE factor = 8; FOV = 3 × 3 × 1.5 cm; matrix 128 × 128 × 64) in which T1 weighting was introduced into the MR images using an inversion pulse (inversion time was set at 1100 ms, sufficient to allow canceling of the embedding gel) or a 3D-gradient echo sequence (TR = 110 ms; TE = 3 ms; $\alpha = 60°$; FOV = 3 × 3 × 1.5 cm; matrix 128 × 128 × 64).

2.7 *In vitro* cytocompatibility

Murine fibroblasts cells (designated L929) were used to assess the *in vitro* cytocompatibility of the materials as recommended by the International and European Standards (ISO 10993-5:2009). L929 cells were cultured in DMEM alpha supplemented with 10 % Fetal Bovine Serum (FBS), penicillin (100 U/mL), streptomycin (100 µg/mL) and glutamine (2 mM). Sample disks (ø 15 mm) were cut from copolymer films and disinfected in ethanol for 30 minutes before immersion in a solution of sterile PBS containing penicillin and streptomycin (1 mg/mL) and incubation for 48 hours at 37 °C. Films were then rinsed 2 times with sterile PBS before soaking for 12 hours in sterile PBS. After disinfection, disks were placed in TCPS 12-well plates and Viton® O-rings were used to maintain the samples on the bottom of the wells and avoid cells growing on TCPS underneath the samples. Disks were finally seeded with 1.10^4 cells and viability was evaluated after 1, 2 and 3 days using PrestoBlue® assay, which reflects the number of living cells present on a surface at a given time point. At scheduled time points, culture medium was removed and replaced by 1 mL of fresh medium containing 10 % of PrestoBlue®. After 2 hours of incubation at 37 °C, 200 µL of supernatant were taken from each well and analyzed for fluorescence at 530 nm (ex.) and 615 nm (em.) with a Victor X3 (Perkin Elmer).

3. Results and discussions

3.1 Synthesis of the PCL MMCAs

The objective of the present work was to propose an alternative strategy to hydrophilic MMCAs or mixtures of low molecular weight CAs and polymer matrices for the preparation of MRI-visible nanoparticles. In addition, attention was paid to provide MRI-visible nanoparticles that would also be degradable and biocompatible. Therefore, two multivalent hydrophobic PCL MMCAs have been prepared (Scheme 1).

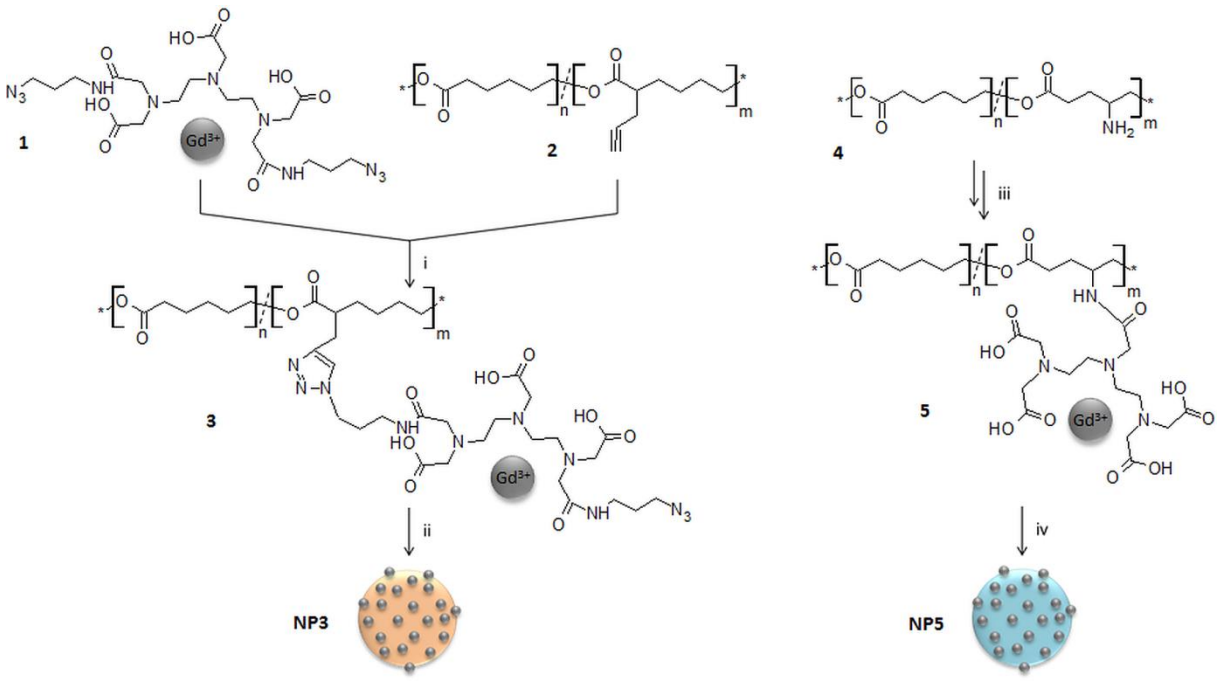

Scheme 1. Preparation of MRI-visible PCL nanoparticles : i) CuBr, PMDETA, DMF, RT, 48 hours ; ii) (PCL, **2**, SPAN®80, acetone) / (Tween®80, water), RT, 2 hours ; iii) DTPA dianhydride, Et_3N, DMF_{an}, RT, 24 hours and $GdCl_3$-$6H_2O$, DMSO, 40 °C, 4 days ; iv) (PCL, **5**, SPAN®80, acetone) / (Tween®80, water), RT, 2 hours.

In a first approach, the ligation chemistry between the PCL backbone and the Gd(III) chelate was based on azide-alkyne Huisgen cycloaddition. An azide-functionalized bis-amide DTPA(Gd(III)) chelate (**1**) and PCL-yne (**2**) have been prepared and used for the CuAAC according to a previously reported methodology.[29] Thanks to the high efficiency of the click chemistry ligation and of the use of a preformed clickable Gd(III) chelate, this strategy allows to finely tune the final Gd(III) content as well as the density of Gd(III) chelate along the polymer backbone. To ensure MRI-visibility of the targeted MMCA, a PCL containing 5 mol% of propargylated units (Mn_{SEC} = 25000 $g.mol^{-1}$. Đ= 1.9) was synthesized and conjugated to the azide-functionalized bis-amide DTPA(Gd(III)). This composition was chosen to yield a final Gd(III) content of ca. 2 wt%, as it was shown in previous studies that this ratio provides a good MRI signal enhancement while minimizing the overall loading of

the toxic Gd(III) species.[29] The copolyesters were characterized before and after ligation by ^{1}H NMR analyses (Supporting Information Figure S1). The final content of Gd(III) in **3** was determined by ICP-MS and found to be 2.6 wt% in the copolyester to be compared with the targeted 2.1 wt%. This small discrepancy may be due to an initial underestimation of the propargyl group content, resulting from the low intensity of the signal corresponding to the methine proton of the propargyl in the ^{1}H NMR spectra.

In a second approach, the ligation chemistry between the PCL backbone and the Gd(III) chelate was based on the reaction between the primary amine groups of poly(ε-caprolactone-co-5-amino-δ-valerolactone)[36,37] (P(CL-co-NH_2VL)) and the activated carboxylic groups of DTPA dianhydride to yield an original Gd(III)/PCL amide conjugate. P(CL-co-NH_2VL) (**4**) was synthesized by ring opening polymerization of εCL and amino-protected 5-Z-amino-δ-valerolactone (NHZ-VL), followed by the acidic recovery of the free amine groups. The molar ratio of NH_2-VL was 33% while the final molecular weight was Mn_{SEC} = 6000 g.mol^{-1} with Đ= 1.2 (Supporting Information Figure S2a). In opposition to the first strategy, the PCL MMCA was obtained in two steps by reaction of **4** with the Gd(III) ligand, namely DTPA dianhydride, and the subsequent complexation of the macromolecular ligand with $GdCl_3$-$6H_2O$. ^{1}H NMR analysis was used to evaluate the extent of DTPA grafting on **4** (Supporting Information Figure S2b). By comparison between the intensities of the signals at δ = 3.0 to 3.50 ppm corresponding to the methylene protons of mono-amide DTPA and of the methine proton of NH_2-VL units and the signal at δ = 4.00 ppm corresponding to the methylene protons of εCL and NH_2-VL units, a 60% yield was calculated. **5** was finally obtained by complexation of $GdCl_3$-$6H_2O$ with the PCL macroligand. The final content of Gd(III) in **5** was determined by ICPMS and found to be 15.4 wt% in good accordance with the expected value of 14.7 wt%.

3.2 In vitro cytocompatibility of PCL MMCAs

Tests were conducted on the L-929 fibroblasts cell line, as recommended by International and European standards.[38] Cytocompatibility of the MRI-visible polymers was assessed on films containing the same gadolinium concentration (0.1 wt%) as the one used in the MRI-visible nanoparticles (see 3.3 and 3.4). In addition, higher concentrations (0.4 wt% and 1 wt%) were also evaluated for films prepared with **5** as this MMCA was evaluated for the first time. Cell proliferation and its extent were compared with TCPS culture plates and PCL films controls. As shown in Figure 1 the presence of PCL MMCAs **3** and **5** did not impede fibroblast proliferation. At a 0.1wt% Gd(III) concentration, similar results were observed for **3** and **5** although their chemical nature and ligation strategies were different. Although lower than on TCPS control, proliferations occurred on films prepared with **3** or **5**. They were similar, if not higher, to the ones observed on pristine PCL, which is widely recognized as a biocompatible material. The same trend was observed for films prepared from **5** and having a higher (0.4 wt%) Gd(III) concentration. Only at the high 1.0 wt% Gd(III) concentration a lower proliferation was observed. Two conclusions may be pointed out from these results. First, concentrations of Gd(III) should be kept low to guaranty a maximal cytocompatibility. This should not be a problem considering the good MRI-visibility obtained with the lowest 0.1 wt% Gd(III) concentration (see 3.4). Secondly, taking into account the similar proliferation obtained with MRI-PCLs compared to PCL, the former would appear to be suitable for the growth of fibroblasts and cell-contacting applications.

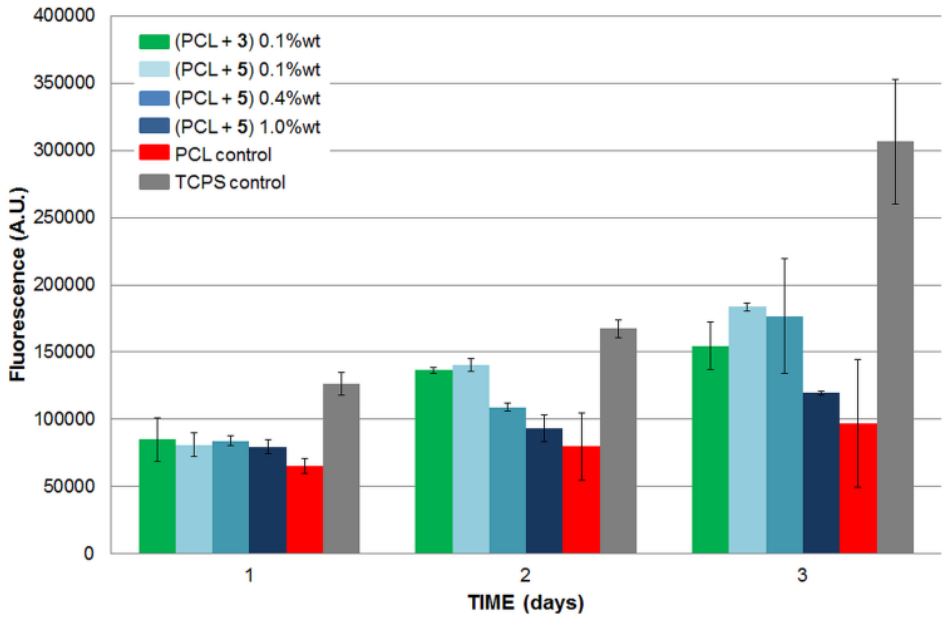

Figure 1. L929 proliferation on PCL MMCAs films compared to PCL films and TCPS (positive control) (data are expressed as means ± SD and correspond to measurements in triplicate).

3.3 MRI-visible nanoparticles

Nanoparticles were prepared by nanoprecipitation with acetone and water as a miscible solvents mixture. An overall concentration of Gd(III) equal to 0.1 wt% was targeted and obtained by mixing defined amounts of pristine PCL and MRI-visible PCLs **3** and **5**. In addition to MRI-visible nanoparticles **NP3** and **NP5**, control PCL nanoparticles were also prepared. Dynamic light scattering (DLS) measurements showed diameter of nanoparticles ranging from 120 to 170 nm with polydispersities around 0.250 (Table 1, Figure S3). The distribution of nanoparticles obtained by DLS was in agreement with the one reported in the literature under the same conditions.[39] Images obtained by TEM show spherical nanoparticles with a moderate size-distribution (Figure 2). Image analyses gave relatively smaller diameters compared to DLS measurements, typically in the range 55 to 80 nm. This difference is attributed to the presence of few larger nanoparticles aggregates (see Figure S4) that may

form as a result of the hydrophobicity of the PCL nanoparticles and that are known to influence DLS measurements in the intensity mode.

Table 1. Mean particle size and zeta potential of PCL and MRI-visible PCL nanoparticles.

Particles	Mean particle size [nm]	PDI[a]	Zeta Potential [mV]		Gd/PCL [wt%]
			mQ water	PBS	
PCL	123 ± 6[a] (55 ± 15)[b]	0.236 ± 0.012	-38	-5	0
P(CL[DTPA(Gd)]) **NP3**	153 ± 11[a] (71 ± 18)[b]	0.276 ±0.016	-46	-8	0.1
P(CL-co-VL[DTPA(Gd)]) **NP5**	170 ± 24[a] (80 ± 20)[b]	0.246 ±0.055	-25	-9	0.1

[a] Determined by DLS ; [b] Determined by TEM image analysis

Zeta potential of the nanoparticles was measured for all systems in milliQ water and in PBS (Table 1). All nanoparticles had a negative zeta potential with values ranging from -46 mV to – 25 mV in water and from -9 mV to -5 mV in PBS. These negative values are classically observed for PCL nanoparticles, likely due to the surface exposure of carboxylate groups of the chain-ends at the surface.[40] In addition, in **NP3** and **NP5** the mono-amide DTPA carboxylic groups are also exposed. The presence of bis-amide DTPA in copolymer **3** decreased the zeta potential of **NP3** compared to PCL nanoparticles as shown by a ca. 10 mV decrease. In opposition, the presence of partially protonated amine groups in PCL-co-VLDTPA(Gd) resulted in a shift of the zeta potential of **NP5** towards less negative values, with a 10 mV increase compared to PCL. Upon addition of salts in PBS medium and as a result of charge screening, zeta potential values drifted towards more neutral values while remaining negative.

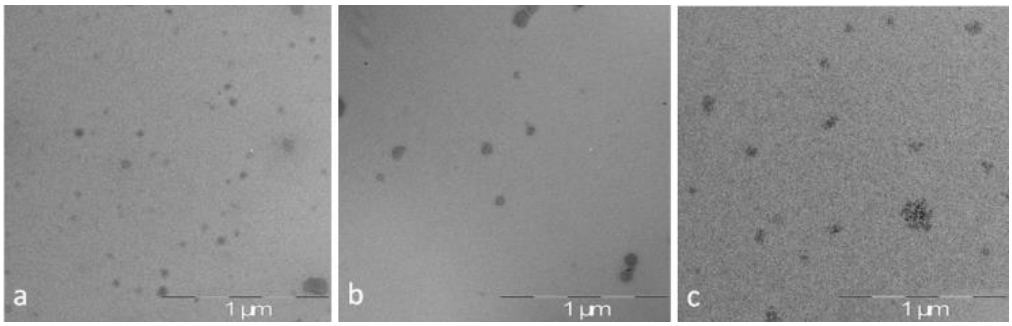

Figure 2. TEM micrographs of (a) PCL nanoparticles (b) P(CL[DTPA(Gd)]) nanoparticles **NP3** and (c) P(CL-co-VL[DTPA(Gd)]) nanoparticles **NP5**.

3.4 Nanoparticles MRI-visibility

MRI-visibility of the nanoparticles (0.1 wt% of Gd(III)) was evaluated by embedding them in agarose gel prior to MRI experiments. **NP3** and **NP5** showed a positive T1 signal enhancement both in spin-echo (SE) (Figure 3a) and gradient-echo (GE) sequence (Figure 3b), which is of importance when considering that GE sequences are clinically used. The longitudinal relaxation times T1 of the water protons in the surroundings of the nanoparticles were first measured. They were found equal to 310 ms in the surrounding of **NP3** and 890 ms in the surrounding of **NP5,** to be compared to 2500 ms for the water protons in the genuine gel. It is remarkable that with concentrations of Gd(III) as low as 0.1 wt% the particles were highly visible. This confirms that hydrophobic PCL MMCAs may allow MR imaging with low Gd(III) concentration compared to the current clinical bolus injections of commercial DTPA/Gd(III) contrast agents (0.1 mmol/kg). It should be noted that no direct comparison between T1 and relaxivities of the MRI-visible nanoparticles and of conventional water soluble small molecular weight DTPA/Gd(III) contrast agents was considered. Indeed, as a direct consequence of their hydrophobic nature, aggregates of **NP3** and **NP5** were found in the gel, which bans these studies that are based on concentration dependent analyses of homogeneous aqueous solutions or dispersions. However, it is possible to compare the longitudinal relaxation times T1 measured in the surrounding of the nanoparticles with the

one of DTPA/Gd(III) solutions. T1 for **NP3** (310 ms) and **NP5 (**890 ms) roughly corresponds to T1 of 1.6 mmol/L and 0.8 mmol/L solution of DTPA/Gd(III), respectively, which corresponds to concentrations used in clinic.[2] In the frame of further studies, dual modification of functional PCLs with DTPA derivatives and low extents of poly(ethylene oxide) chains should be considered to allow the nanoparticles dispersion without aggregation while guarantying the overall hydrophobic character of the polymers.

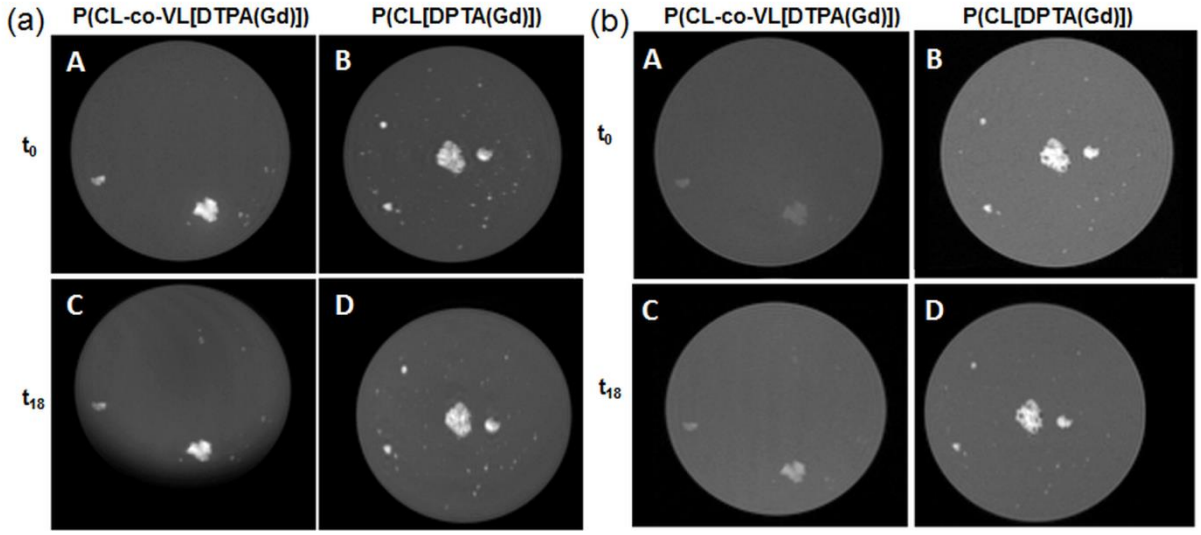

Figure 3. Spin echo (a) and gradient echo (b) MR-imaging at t_0 and after 18 months storage. (A-C) P(CL-co-VL[DTPA(Gd)]) nanoparticles **NP5** aggregates; (B-D) P(CL[DTPA(Gd)]) nanoparticles **NP3** aggregates (MRI field 7 Teslas).

MR imaging was finally carried out on the same samples after storage for a prolonged period of 18 months at 4°C. Lower rows in Figure 3a and 3b show the signal observed for **NP3** and **NP5** after storage. It is to note that under the same MRI experiment conditions, the T1 signal enhancement was similar to the one initially observed. Moreover, as the signal of the gel did not significantly change with time and that no diffusion in the gel was observed, it may be assumed that no release of Gd(III) occurred, which qualitatively confirms the stability of the macromolecular contrast agents. Of course under physiological conditions different results

may be expected, but this result is in agreement with a previous study carried out on films prepared with compound **3** that demonstrated a good stability at 37°C (PBS, pH 7.4) with only 0.1% of the total amount of Gd(III) released after 6 months from films.[29]

4. Conclusion

In this work we reported on two hydrophobic and degradable PCL MMCAs that were successfully synthesized for the straightforward preparation of MRI-visible nanoparticles. The two strategies, convergent click chemistry and divergent amidification, led to MMCAs suitable for the preparation of MRI-visible nanoparticles containing 0.1wt% Gd(III) and exhibiting hydrodynamic diameters in the range 120 to 170 nm. Although different in nature, all nanoparticles turned to be MRI-visible independently of the MRI sequence used, in particular when using the clinically relevant gradient-echo sequence. Although this first study should be completed in the near future by additional experiments (degradation assays, toxicity evaluation of NP, hydrophilization of NP surfaces, in vitro/in vivo evaluation), we believe that the proposed PCL MMCAs represent an attractive platform for the preparation of degradable theranostic agents and could open the way to new diagnostic tools.

Acknowledgements

The authors wish to thank the French Ministry of Education and Research for Sarah El Habnouni’s fellowship, the Erasmus program for Barbara Porsio's fellowship. For analyses, authors thank Chantal Douchet and Olivier Bruguier for ICP-MS, Corine Tourné-Péteilh for Nano ZS, Sylvie Hunger and Cedric Paniagua for NMR and Frank Godiard for TEM.

References

1 M. Rudin and R. Weissleder, *Nat. Rev. Drug Discov.* 2003, **2**, 123-131.

2 Y. Zhang, J. Zhou, D. J. Guo, M. Ao, Y. Y. Zheng and Z. G. Wang, *Int. J. Nanomed.* 2013, **8**, 3745-3756.

3 P.W. Lee, S.H. Hsu, J.J. Wang, J.S. Tsai, K.J. Lin, S.P. Wey, F.R. Chen, C.H. Lai, T.C. Yen, H.W. Sung, *Biomaterials* 2010,**31**, 1316-1324.

4 V. V. Mody, M. I. Nounou and M. Bikram, *Adv. Drug Deliver. Rev.* 2009, *61*, 795-807.

5 S. Aime, D. D. Castelli, S. G. Crich, E. Gianolio and E. Terreno, *Acc.Chem. Res.* 2009, **42**, 822-831.

6 K. Shiroishi and M. Yokoyama, *Drug Deliver. Syst.* 2008, **23**, 33-39.

7 P. Caravan, *Chem. Soc. Rev.* 2006, **35**, 512-523.

8 V. P. Torchilin, *Adv. Drug Deliver. Rev.* 2002, **54**, 235-252.

9 A. J. L. Villaraza, A. Bumb and M. W. Brechbiel, *Chem. Rev.* 2010, **110**, 2921-2959.

10 M. G. Duarte, M. H. Gil, J. A. Peters, J. M. Colet, L. Vander Elst, R. N. Muller and C. F. G. C. Geraldes, *Bioconjugate Chem.* 2001, **12**, 170-177.

11 T. L. Kaneshiro, T. Ke, E. K. Jeong, D. L. Parker and Z. R. Lu, *Pharm. Res.* 2006, **23**, 1285-1294.

12 I. Pashkunova-Martic, C. Kremser, M. Galanski, P. Schluga, V. Arion, P. Debbage, W. Jaschke and B. Keppler, *Mol. Imaging Biol.* 2011, **13**, 432-442.

13 Y. Zong, J. Guo, T. Ke, A. M. Mohs, D. L. Parker and Z. R. Lu, *J. Control. Release* 2006, **112**, 350-356.

14 F. Fernandez-Trillo, J. Pacheco-Torres, J. Correa, P. Ballesteros, P. Lopez-Larrubia, S. Cerdan, R. Riguera and E. Fernandez-Megia, *Biomacromolecules* 2011, **12**, 2902-2907.

15 Y. J. Fu, H. J. Raatschen, D. E. Nitecki, M. F. Wendland, V. Novikov, L. S. Fournier, C. Cyran, V. Rogut, D. M. Shames and R. C. Brasch, *Biomacromolecules* 2007, **8**, 1519-1529.

16 X. J. Li, Y. F. Qian, T. Liu, X. L. Hu, G. Y. Zhang, Y. Z. You and S. Y. Liu, *Biomaterials* 2011, **32**, 6595-6605.

17 Y. Li, M. Beija, S. Laurent, L. vander Elst, R. N. Muller, H. T. T. Duong, A. B. Lowe, T. P. Davis and C. Boyer, *Macromolecules* 2012, **45**, 4196-4204.

18 W.-L. Zhang, N. Li, J. Huang, J.-H. Yu, D.-X. Wang, Y.-P. Li and S.-Y. Liu, *J. Appl. Polym. Sci.* 2010, **118**, 1805-1814.

19 Z. Zheng, A. Daniel, W. Yu, B. Weber, J. Ling and Axel H. E. Müller, *Chem. Mater.*, 2013, **25**, 4585-4594.

20 M. Ye, Y. Qian, Y. Shen, H. Hu, M. Suia and J. Tang, *J. Mater. Chem.* 2012, **22**, 14369-14377.

21 A. Beilvert, D. P. Cormode, F. Chaubet, K. C. Briley-Saebo, V. Mani, W. J. M. Mulder, E. Vucic, J. F. Toussaint, D. Letourneur and Z. A. Fayad, *Magn. Reson. Med.* 2009, **62**, 1195-1201.

22 M. Grogna, R. Cloots, A. Luxen, C. Jerome, C. Passirani, N. Lautram, J. F. Desreux and C. Detrembleur, *Polym. Chem.* 2010, **1**, 1485-1490.

23 H. Y. Lee, H. W. Jee, S. M. Seo, B. K. Kwak, G. Khang and S. H. Cho, *Bioconjugate Chem.* 2006, **17**, 700-706.

24 E. D. Pressly, R. Rossin, A. Hagooly, K. I. Fukukawa, B. W. Messmore, M. J. Welch, K. L. Wooley, M. S. Lamm, R. A. Hule, D. J. Pochan and C. J. Hawker, *Biomacromolecules* 2007, **8**, 3126-3134.

25 K. Shiraishi, K. Kawano, T. Minowa, Y. Maitani and M. Yokoyama, *J. Control. Release* 2009, **136**, 14-20.

26 G. D. Zhang, R. Zhang, X. X. Wen, L. Li and C. Li, *Biomacromolecules* 2008, *9*, 36.

27 I. Perez-Baena, I. Loinaz, D. Padro, I. Garcia, H. J. Grande and I. Odriozola, *J. Mater. Chem.* 2010, **20**, 6916-6922.

28 S. Blanquer, O. Guillaume, V. Letouzey, L. Lemaire, F. Franconi, C. Paniagua, J. Coudane and X. Garric, *Acta Biomater.* 2012, **8**, 1339-1347.

29 S. El Habnouni, B. Nottelet, B. Porsio, V. Darcos, L. Lemaire, F. Franconi, X. Garric and J. Coudane, *Biomacromolecules* 2013, **14**, 3626.

30 O. Guillaume, S. Blanquer, V. Letouzey, A. Cornille, S. Huberlant, L. Lemaire, F. Franconi, R. de Tayrac, J. Coudane and X. Garric, *Macromol. Biosci.* 2012, **12**, 1364-1374.

31 A. Z. Faranesh, M. T. Nastley, C. P. de la Cruz, M. F. Haller, P. Laquerriere, K. W. Leong and E. R. McVeigh, *Magn. Reson. Med.* 2004, **51**, 1265-1271.

32 H. H. Chen, C. Le Visage, B. S. Qiu, X. Y. Du, R. Ouwerkerk, K. W. Leong and X. M. Yang, *Magn. Reson. Med.* 2005, **53**, 614-620.

33 A. L. Doiron, K. Chu, A. Ali and L. Brannon-Peppas, *P. Natl. Acad. Sci. USA.* 2008, **105**, 17232-17237.

34 B. C. M. te Boekhorst, L. B. Jensen, S. Colombo, A. K. Varkouhi, R. M. Schiffelers, T. Lammers, G. Storm, H. M. Nielsen, G. J. Strijkers, C. Foged and K. Nicolay, *J. Control. Release* 2012, **161**, 772-780.

35 G. Ratzinger, P. Agrawal, W. Koerner, J. Lonkai, H. M. H. F. Sanders, E. Terreno, M. Wirth, G. J. Strijkers, K. Nicolay and F. Gabor, *Biomaterials* 2010, **31**, 8716-8723.

36 S. Blanquer, J. Tailhades, V. Darcos, M. Amblard, J. Martinez, B. Nottelet and J. Coudane, *J. Pol. Sci.-Polym. Chem.* 2010, **48**, 5891-5898.

37 B. Nottelet, M. Patterer, B. Francois, M. A. Schott, M. Domurado, X. Garric, D. Domurado and J. Coudane, *Biomacromolecules* 2012, **13**, 1544-1553.

38 AFNOR, 2009, ISO 10993-5:2009.

39 Z. Zili, S. Sfar and H. Fessi, *Int. J. Pharm.* 2005, **294**, 261-267.

40 Y. Ma, Y. Zheng, X. Zeng, L. Jiang, H. Chen, R. Liu, L. Huang, L. Mei, *Int. J. Nanomed.* 2011, **6**, 2679-2688.

Table of Contents